Chapter-4

Chapter 4

Thermal and Mechanical Properties of Functionalized Poly(vinyl chloride)/Layered double hydroxide Nanocomposites

4.1 Introduction

The main objective of advanced material research is to synthesize and characterize new material. Interdisciplinary nature of polymer composites play vital role in this area because it brings together biology, material science and nanotechnology at one place. Their intercalation technology offers new area for developing nanohybrids with desired functionality. The interaction between nano filler component of nanocomposites at the nanoscale enables them to act as molecular bridges in the polymer matrix [Hule et al. (2007)].

The properties of composite material are greatly influenced by the amount of substance between the two materials. Polymer nanocomposites are the combination of polymer and nanomaterial at the nanoscale. These materials exhibit multifunctional and high-performance characteristics just by adding a small amount of nanoparticle in the polymer matrices. These materials demonstrate special performance from conventional materials with micro scale structure, due to their high surface area, hydrophilic character and low cost [Ishida et al. (2000)]. The study of polymer nanocomposites has been a very active area of research because very small amount of clay brings about large enhancement in the mechanical properties [Ray et al. (2003)], thermal properties [Usuki et al. (1993)], optical [Liu et al. (2008)] and gas permeability [Turhan et al. (2010); Kojima et al. (1993)]. Govinda et al. 2012 have demonstrated that bone cement/LDH

hybrid exhibit substantial improvement in mechanical and thermal properties and make possible new material application in biomedical field [Govinda et. al. (2012)].

Poly vinyl chloride (PVC), synthetic polymeric materials have been widely used in biomedical applications as clinical analysis of salt, blood storage, catheters [Lee *et al.* (2000)]. Its mechanical property and excellent capability to acquire desired functional group makes it a choice of research in polymer field since its discovery in 19^{th} centaury [Braun et al. (2004)]. Several reports to improve the biocompatibility of PVC have been reported in literature [Balakrishnan et al. (2005); James et al. (2003)].

Layered double hydroxide (LDH) represent a layered structure consisting of di- and trivalent metal cations [M(II) and M(III)] coordinated by interlayer anion. The substitution of M(III) cations induces an overall positive charge that is counterbalanced by exchangeable interlayer anions. Thus, LDH can serve as host for polymeric intercalation [Costa *et al.* (2008)]. The structure of LDHs is represented by the general formula of

$$[M^{2+}_{1-x}\, M^{3+}_{x}\, (OH)_2]^{x+}\, (A^{n-})_{x/n}]\cdot mH_2O$$

where M^{2+} and M^{3+} can be any divalent and trivalent metal ions (whose ionic radius is not so different from that of Mg^{2+}), which can be accommodated in the octahedral sites in the brucite-like layers and x is the metal ratio $M^{3+}/(M^{2++}M^{3+})$.

A^{n-} in the interlamellar region can be any anion (organic or inorganic) and m is the amount of water in mol, present in the same region. The amount of water in the interlayer region can be determined by factors such as the nature of the anions, the water vapour pressure and temperature [Nalawade et al. (2009)].

Polymer/clay nanocomposite preparation proposes a new approach in the presence of high performance nanoclay. Polymer nanocomposite has an ability to afford exfoliation/ intercalation phenomenon which provide enhancement of mechanical properties [Wan et al. (2003)]. LDH based polymer composites have been paying attention on natural occurring materials such as clay. In recent years, researchers have been attracted toward synthetic clay (LDH) due to their structure similarity with natural clay, for example (PVC)/montmorillonite (MMT) for improved mechanical properties [Liu et al. (2003)]. LDH are identified for their application in pharmaceutics [Aguzzi et

al. (2007)] and for providing excellent active biological properties including biocompatibility and less cytotoxicity [Choy Liu et al. (2000)].

In the present work, LDH composite of functionalized PVC was prepared with thiosulphate, thiourea and sulphate and further prepared their polymer composite with varying percentage of LDH. Characterization studies of PVC, LDH and their composite were carried out by X-ray diffraction (XRD); the interaction between LDH and PVC through FTIR; the optical properties were determined using UV-vis spectrophotometer; the thermal stability was determined by means of TGA.

4.2 Result and discussion

4.2.1 Nanostructure of LDH

The FT-IR and XRD characterization technique are very supportive for the study of layered double hydroxides. The synthesized LDHs including Mg_2Al-LDH-CO_3 prepared by co-precipitation method are characterized by FTIR techniques and XRD (Figure 4.1). In FTIR (Figure 4.1(a)) spectra of prepared LDHs have a broad absorption band around 3051 cm^{-1} is assigned to O-H interlayer water with interlayer CO_3^{-2} anions. The band at 1644 cm^{-1} is due to bending vibration of interlayer water.

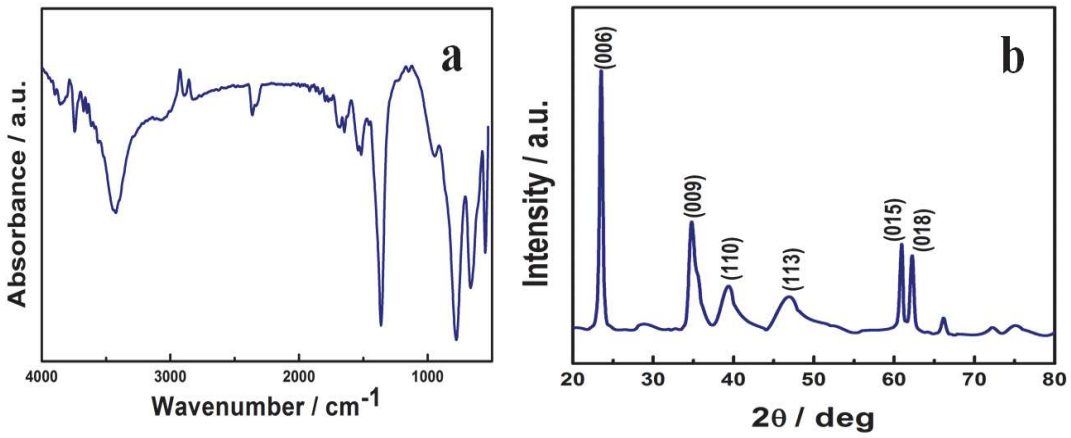

Figure 4.1: (a) FTIR and (b) XRD patterns of MgAl-CO_3 LDH with Mg/Al Molar ratio 2:1.

A strong peak at 1366 cm^{-1} is associated with the asymmetric stretching vibration of the carbonate anions. M-OH stretching was observed in fingerprint region at 551 and 45 cm^{-1} [Govinda et al. (2012)]. Bao et. al. (2005) synthesized LDH-CO_3 and LDH-DS for PVC/LDH composites and Wang et al. (2006) also found comparable result when prepared LDH for synthesizing LDHs/PMMA composites.

The sharp and distinct peak observed in XRD pattern for the Mg-Al-CO_3-LDH showed the highly crystalline nature and layered geometry phase. Figures 4.1 (b) shows a chain of sharp peak that is characteristic of an ordered layer structure of Mg_2Al-LDH-CO_3. The obtained plane (006), (009), (010), (013), (015), and (018) counter to diffraction peak at 2θ = 23.5°, 34.6°, 38.9°, 46.1°, 62.2° and 66.1° validate the hexagonal structure of LDHs.

4.2.2 Fourier Transform Infrared spectroscopy

FTIR spectra of polymeric PVC and functionalized PVC have been reported in previous chapters. All functionalized PVC composites of 1, 1.5 and 2% having the distinct absorption peak around 3100-3500 cm^{-1} are attributed to the O–H stretching modes of interlayer water molecules as well as the hydrogen bonds linked to the interlayer anions. Sharp peaks at ~ 1600 and ~1400 cm^{-1} correspond to asymmetric and symmetric absorption of C-O and C=O in CO_3^{-2} along with multiple peak below 1000 cm^{-1} for Mg/Al-OH stretching absorption [Wang et al. (2006)]. Other than this, presence of thiosulphate in PVC-TS confirms from peak at 1017 cm^{-1} (Figure 4.2 (b)), PVC-TU contains NH stretching observed at 3315 cm^{-1} and 3180 cm^{-1}, 1619 cm^{-1} may be due to N-H bending, while 1425 cm^{-1} for N-C-N stretching confirms PVC-S in Figure 4.2 (c). In case of the all the polymer nanocomposites, the intensity of LDH peaks with high LDH loading has increased. These results support that PVC/LDH nanocomposites are successfully synthesized. Similarly, Liu et al. (2008) also studied different composition of PVC/LDH composite. Similarly, Turhan et al. (2010) synthesized and compared the result of natural and modified kalonite/PVC composites. These results show that different amounts of LDH get dispersed in polymer.

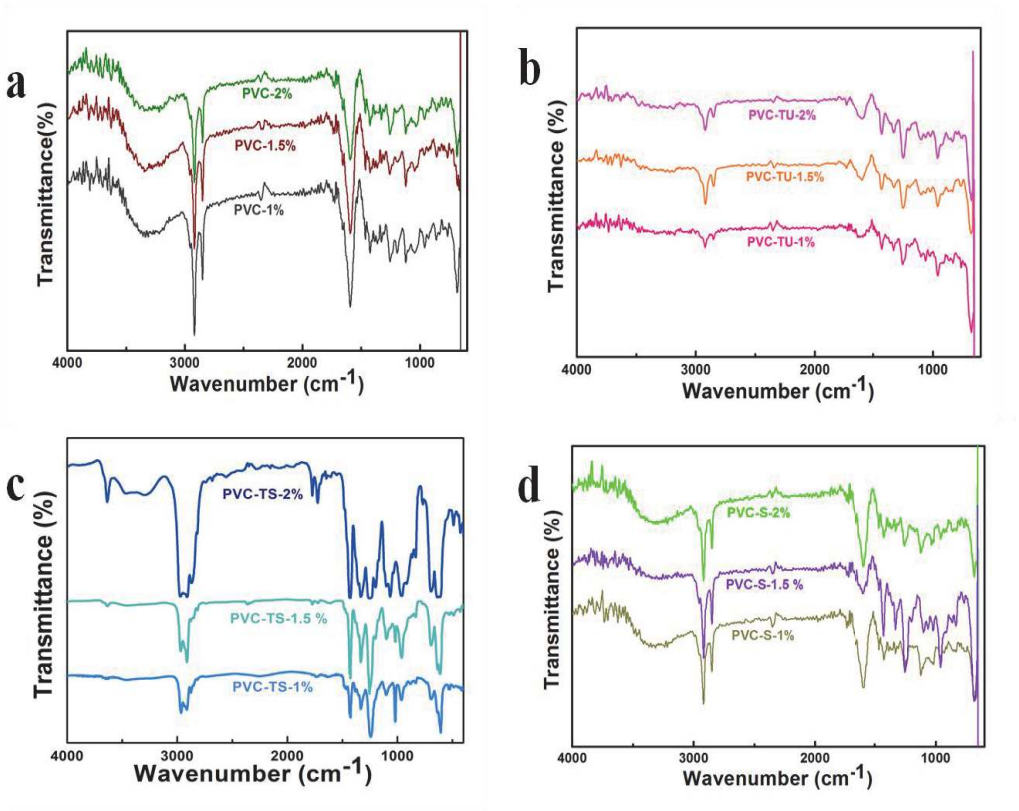

Figure 4.2: (a) FTIR spectra of PVC, PVC-TS, PVC-TS and PVC-S functionalized PVC, (b) PVC-1, 1.5 & 2%, (c) PVC-TS-1, 1.5 & 2%,(d) PVC-TU-1, 1.5 & 2% and (e) PVC-S-1, 1.5 & 2%.

4.2.3 UV-visible spectroscopy

The UV-Vis absorption spectra originated from electronic transitions between ground states to higher energy states, particularly transitiion from σ, π and n to their respective higher energy states of σ*, π* and n*. UV-Vis spectra of the PVC and functionalized PVC composites are shown in Figure 4.3 with the wavelength region of 200-600 nm. The absorbance peak between 200 – 230 nm for is due to to *n*-π* transition where as π-π* transition occurs at 275-290 for all samples due to the presence of carbonyl group in nano material. One absorbance peak was observed in PVC near 206 nm is due to *n*-π* transition but in case of PVC/LDH composites, PVC-1% shifts towards lower wavelength (200 nm) but as we increase the amount of LDH, peak shifts towards the higher wavelength region of 210 nm in PVC-1.5% with 215 nm in PVC-2% (Figure 4.3 (a)).

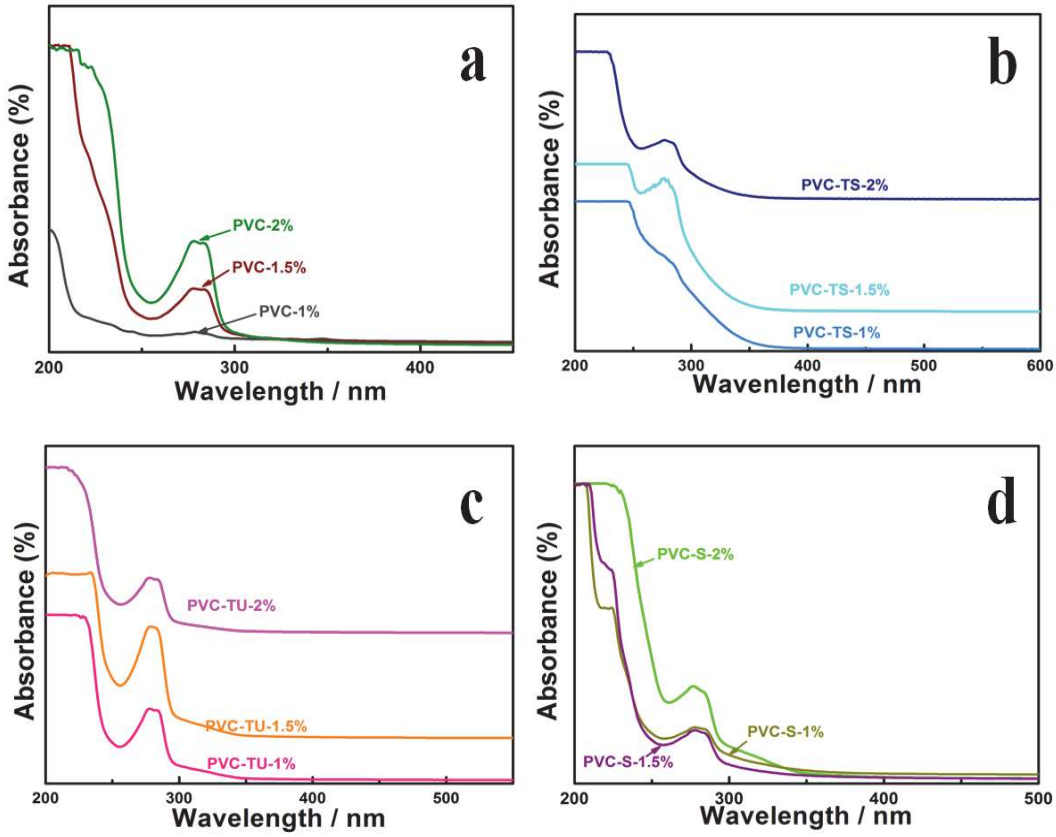

Figure 4.3: (a) UV-visible spectra of PVC and its nanocomposites, (b) PVC-TS and its nanocomposites, (c) PVC-TU and its nanocomposites, (e) PVC-S and its nanocomposites.

PVC-TS/LDH composites show red shifts in all samples compared to PVC-TS (Figure 4.3 (b) as we increase the amount of LDH in polymer matrix. PVC-TS observed a peak at 218 [Monika et al. (2015)] with peak shifting occurring at 246, 244 and 227 nm for PVC-TS-1%, PVC-TS-1.5% and PVC-TS-2%.

While PVC-TU/LDH composites shows the blue shifts as compared to PVC-TU because it has peak at 249 nm [Monika et al. (2015)] other than 229, 233 & 220 nm for PVC-TU-1%, PVC-TU-1.5% and PVC-TU-2% (Figure 4.3 (c)). Similarly, 209, 206, 208 and 225 nm wavelength observed in PVC-S [Monika et al. (2015)], PVC-S-1%, PVC-S-1.5% and PVC-S-2% (Figure 4.3 (d)).

4.2.4 X-ray diffraction

The dispersed and exfoliated state of LDHs in the polymer matrices was studied by XRD techniques. Figure 4.4 shows the XRD patterns of (a) PVC/LDH, (b) PVC-TS/LDH, (c) PVC-TU/LDH and (d) PVC-S/LDH.

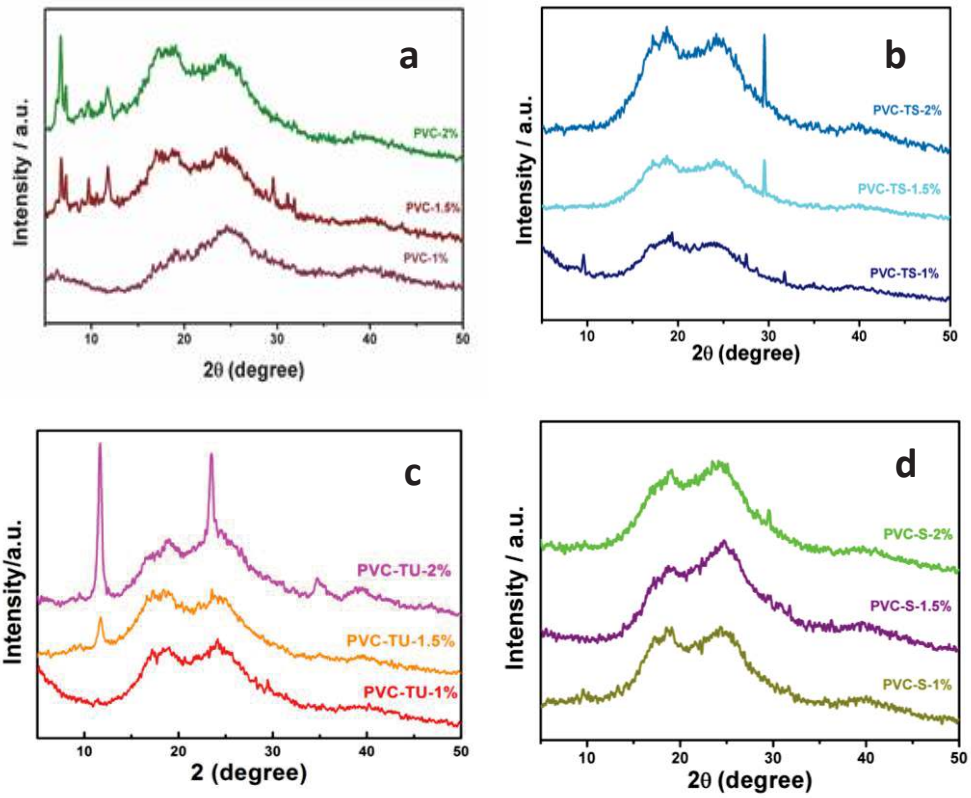

Figure 4.4: (a) XRD of PVC and its nanocomposites, (b) PVC-TS and its nanocomposites, (c) PVC-TU and its nanocomposites, (e) PVC-S and its nanocomposites.

PVC always show two broad diffraction peaks near about at 2θ = 17 and 25 [Liu et al. (2008)]. Along with these PVC peak, PVC-TU/LDH composites confirmed the presence of LDH in its matrix due to presence of their peak at 2θ = 23.4 and 34.5, indicating the intercalation of polymer chain into LDH galleries. But in case of other polymer composites, PVC/LDH, PVC-TS/LDH and PVC-S/LDH, there were LDH peak which demonstrates the dramatic exfoliation of LDH in polymer matrix.

According to the Liu *et al.* 2008, loss of LDH peak below 2θ angle represent that the order of layered structure of nano clay had been greatly destroyed. However, PVC/LDH, PVC-TS/LDH and PVC-S/LDH might be dramatically exfoliated and homogeneous dispersion of LDH in different functional polymer.

4.2.5 Contact angle

Figure 4.5 shows the wettability graph of all the modified and unmodified polymer composites, evaluated by contact angle measurments of synthesized polymer composites in contact with water.

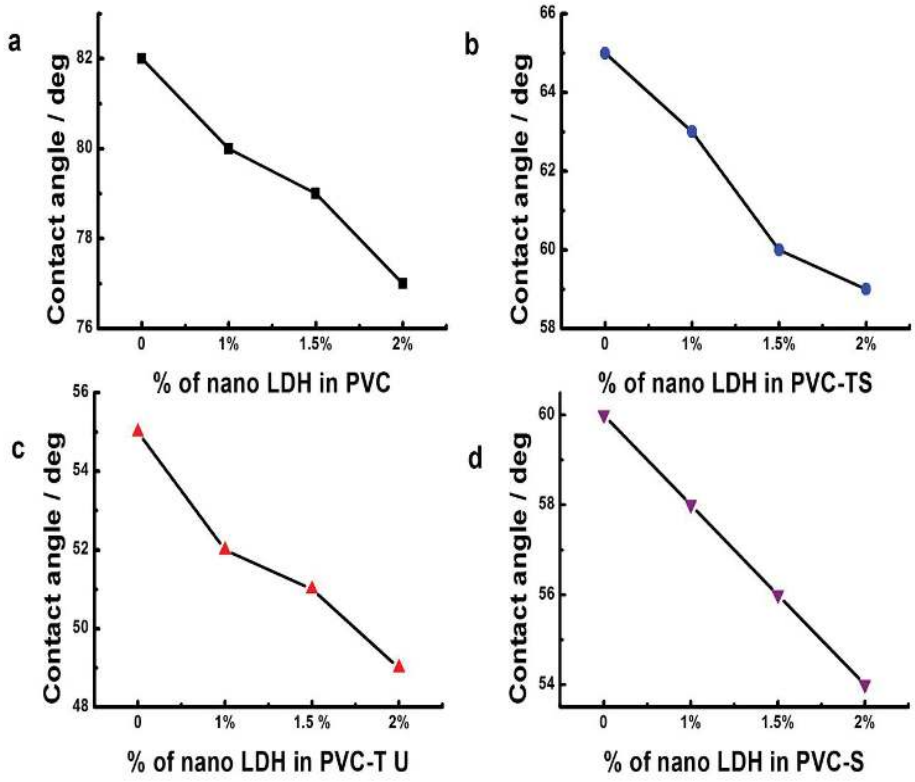

Figure 4.5: Wettability graph of different polymer composites (a) PVC-1, 1.5 & 2%, (b) PVC-TS-1, 1.5 & 2 %, (c) PVC-TU-1, 1.5 & 2% and (d) PVC-S-1, 1.5 & 2%.

The influence of LDH particles in polymer matrix and wettability properties of polymer composite materials were examined and the results are reperented in Figure 4.5. The polymer composites results show significant decrease in the contact angles, indicating

that LDH increases the hydrophilicity of the PVC/LDH composites as well as functional PVC/LDH composites. This is an essential feature in leading the wettability of a material, and it encourages cell growth and proliferation and therby influences the biocompatibility property of polymer composites. Figure 4.5 (a) shows the result of PVC/LDH composites. PVC has contact angle at 82º while after adding 1% LDH it lowers by 2º and after adding 1.5 and 2%, it goes down more showing that the polymer reduces hydrophobicity. PVC-TS shows the 65º before and after addition it shows 63º, 60º & 59º Figure 4.5 (b), PVC-TU shows 55º improved by 52º, 51º & 49º Figure 4.5 (c) and PVC-S shows 60º with enhanced 58º, 56º & 54º Figure 4.5 (d).

4.2.6 Transmission Electron Microscopy

TEM images enable to express the clay inside the polymer. Figure 4.6 shows 2% LDHs in polymer, PVC-TU/LDH (Figure 4.6 (a)) and PVC-S/LDH (Figure 4.6 (b)) image interpret that the polymer nanocomposites have the nanomorphology and LDH clay become more dispersed and exfoliated.

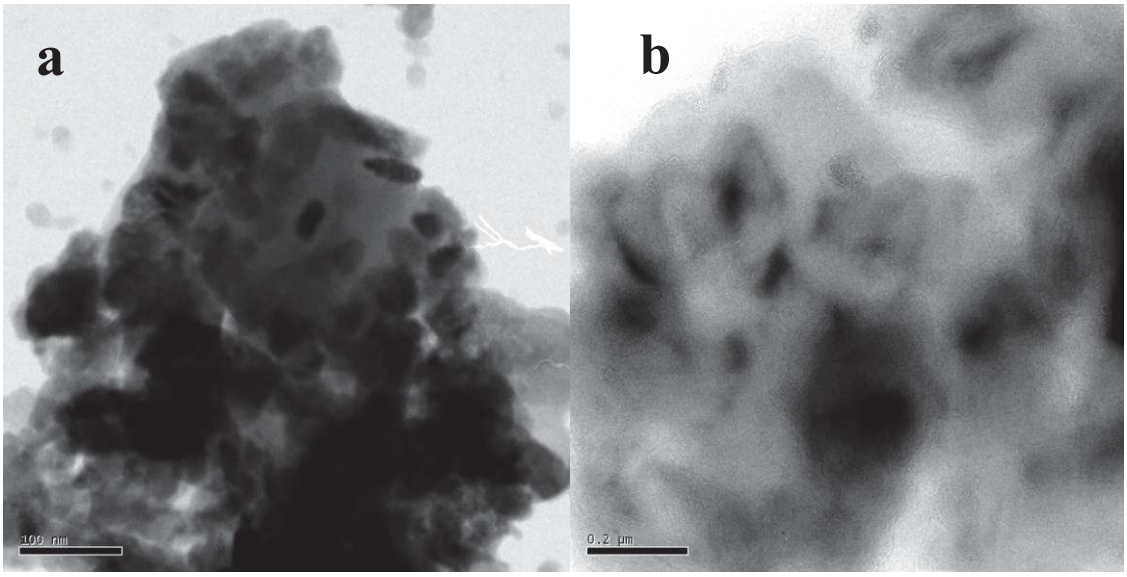

Figure 4.6: TEM images of different polymer composite (a) PVC -2%, (b) PVC-TU-2%.

4.2.7 Thermal analysis

TGA has been used to find out the thermal decomposition of PVC and its derivatives (Figure 4.7). Thermal behaviour of PVC, PVC-TS, PVC-TU & PVC-S has been reported previously. Here, two transition steps can be observed in all the thermograms of polymer composites. The first step corresponds to the weight loss caused by the dehydrochlorination of PVC beginning at temperature of 240^{o}C, while the second transition step represent the total weight loss resulting from the degradation of the dehydrochlorinated residuals [Seeponkai et al. (2013)]. The thermal degradation temperature of functionalized PVC shows differences. The first transition step starts at the onset of PVC-TS, PVC-TU and PVC-S at 200^{o}C, 218.7^{o}C and 190^{o}C respectively, while the second transition step of all functionalized PVC were same as pure PVC.

The thermal degradation temperature of functionalized PVC shifts slightly to lower temperature according to pure PVC. This shows that existence of functional group in the polymer chain encourages the degradation of functionalized PVC. Thermal properties of PVC composites increases after incorporating LDH. All PVC/LDH composite begins dehydrochlorination at 291ºC, it means thermal behaviour increases by 51º. In case of thiosulphated PVC composites, LDH does not put any effect on the polymer because their graph show same pattern like without LDH in PVC-TS. While in case of PVC-TU/LDH composites, it improves from 218ºC to 234ºC compare to pure PVC-TU, it means LDH improved it by 16º.

While PVC-S/LDH composites also improved and become 208ºC from 190ºC compared to pure PVC-S. Along with the first step observation, second transition step near about same (~430) in all polymer composites. LDHs nanoparticle proves that it increases the thermal behaviour of PVC and provides stability to polymer in respect of temperature.

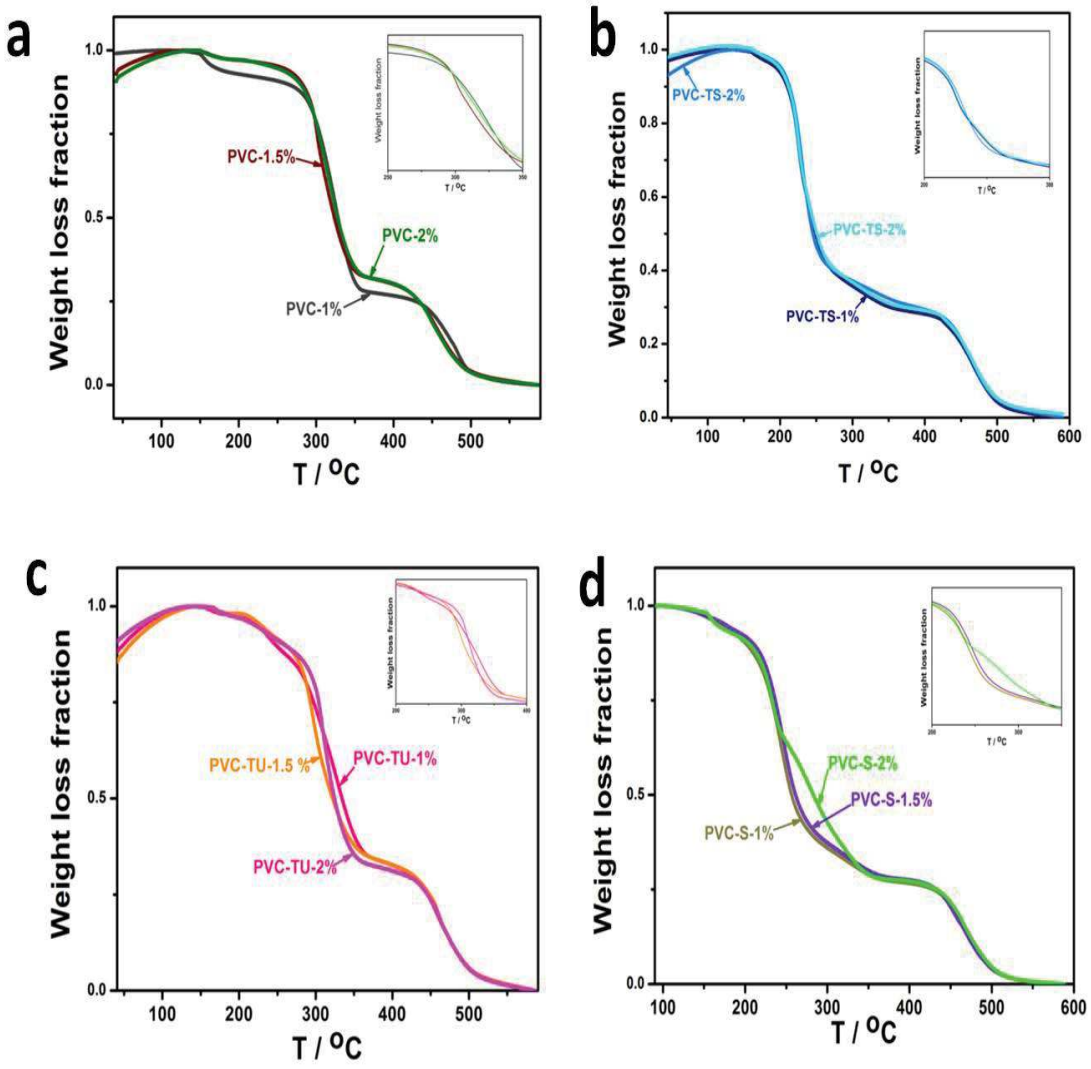

Figure 4.7: Thermograph of polymer composite (a) PVC-1%, PVC-1.5% & PVC-2% (b) PVC-TS-1, PVC-TS-1.5 & PVC-TS-2% (c) PVC-TU-1, 1.5 & 2% (d) PVC-S-1, 1.5 & 2%.

Thermal property of polymer composites did not alter by adding different amounts of LDH. All the results shown above followed same patern in 1, 1.5 & 2% of LDH. [Xue et. al. (2015)] compared different LDH (MgAl-NH_3-LDHs, ZnAl-LDHs & ZnAl--NH_3-LDHs) with plasticized PVC for thermal stability. In addition, Liu et al. (2010) also observed improved thermal stability of PVC/LDH-NO_3, PVC/DS and PVC/LDH-st.

4.2.8 Mechanical properties

Mechanical properties of polymer composites have been shown in different figures 4.8-4.10 with their corresponding polymers and their nanocomposites. Mechanical testing was performed to characterize PVC, functionalized PVC and their polymer nanocomposites with their results summarized in Tabular form (Table 4.1 & 4.2). The data obtained of modulus; toughness and strain at break were also discussed. The tensile testing performed indicated that these nanofibers have modest mechanical properties that can be further improved. However, there is no record of the mechanical properties of these functional PVC and their nanocomposites. Although major improvements are needed to develop effectiove polymer composites with scientific implications, the information presented in this article can be used as a reference for future developments.

Figures 4.8–4.10 designate the influence of the amount of LDH on the yield strength, tensile strength, and the Young's modulus of PVC and functionalized PVC/LDH and their composites, respectively. Figure 4.8 shows stress strain graph of PVC and functionalized PVC with different functional groups. However, sulphate substituted PVC

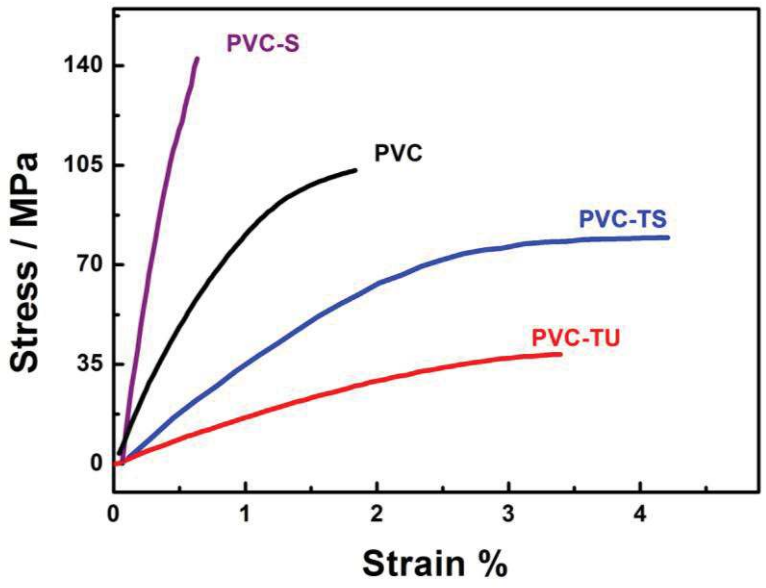

Figure 4.8: Stress strain curve of PVC with functionalized PVC with thiosulphate (PVC-TS), thiourea (PVC-TU) and sulphite(PVC-S).

Table 4.1: Mechanical properties of PVC and different functionalized PVC

Sample	Modulus (GPa)	% Increase in Modulus	Toughness (kJm^{-3})	% Increase in toughness	Ultimate strength (UTS) (MPa)
PVC	107.8	-	124.5	-	103
PVC-TS	36.1	-66.5	232.6	87	79.5
PVC-TU	17.6	-83.6	79.9	-36.2	38.4
PVC-S	320.1	196.9	46.6	-62.5	142

(PVC-S) show better strength, while toughness increases in case of thiosuphate substituted PVC (PVC-TS) by 232 % and their percentage improvements/changes in modulus and toughness are recorded in Table 4.1. Although, functional groups did not effect PVC so much in term of mechanical properties, but nano material has the capacity to change the mechanical behaviour of polymer.

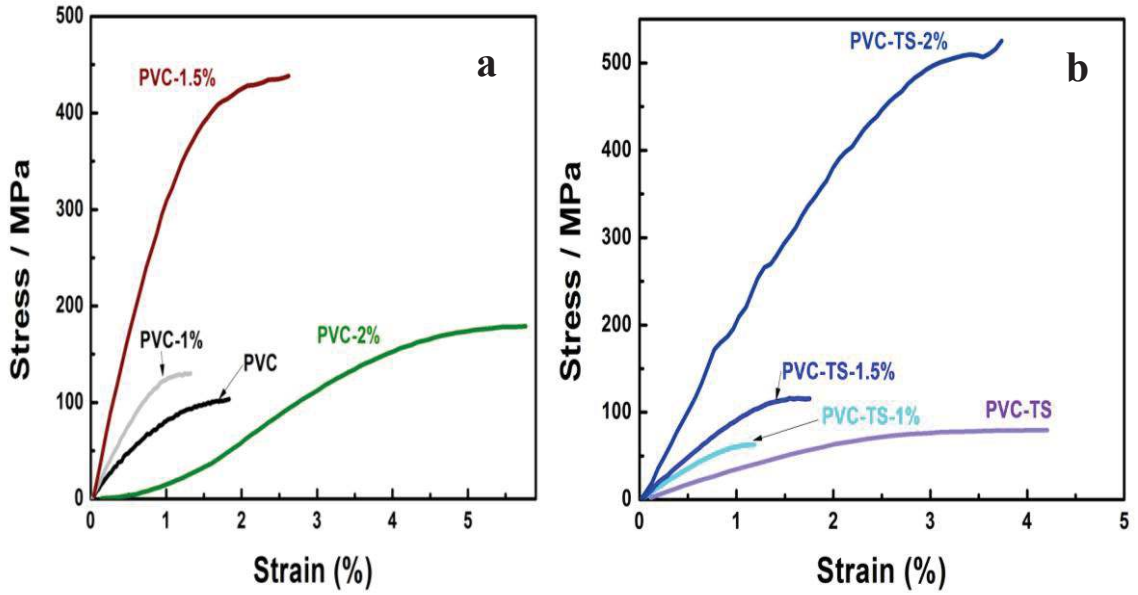

Figure 4.9: Stress strain curve of (a) PVC and its different wt% of LDH nanocomposites; (b) PVC-TS and its different wt% of LDH nanocomposite.

Table 4.2: Mechanical properties of PVC and its nanocomposite.

Sample	Modulus (GPa)	% Increase in Modulus	Toughness (kJm^{-3})	% Increase in toughness	Ultimate strength (UTS) (MPa)
PVC	107.8	-	124.5	-	103
PVC-1%	168.9	57.4	108.4	-16.0	130
PVC-1.5%	360	233.9	813.5	553.5	438.7
PVC-2%	14.3	-86.7	561.7	351.1	178.9

Similarly, Figure 4.9 (a) graph of PVC/LDHs composites and their changes were recorded in Table 4. 2. PVC-1% and 1.5% showed better result compared to pure and functionalized PVC. At the same time, PVC-2% did not perform so well. Figure 4.9 (b) describes about the PVC-TS/LDH nanocomposites, PVC-TS-2% shows very good ultimate strength compared to pure PVC and its composites as well as PVC-TS and its 1% and 1.5% composites.

Table 4.3: Mechanical properties of PVC –TS and its different wt% nanocomposites

Sample	Modulus (GPa)	% Increase in Modulus	Toughness (kJm^{-3})	% Increase in toughness	Ultimate strength (UTS) (MPa)
PVC-TS	36.3	-	232.6	-	79.5
PVC-TS-1%	75.2	107.1	45.2	-80.5	63.0
PVC-TS-1.5%	104.5	187.8	129.3	-44.4	115.6
PVC-TS-2%	227.1	528.5	1214.3	422.0	523.4

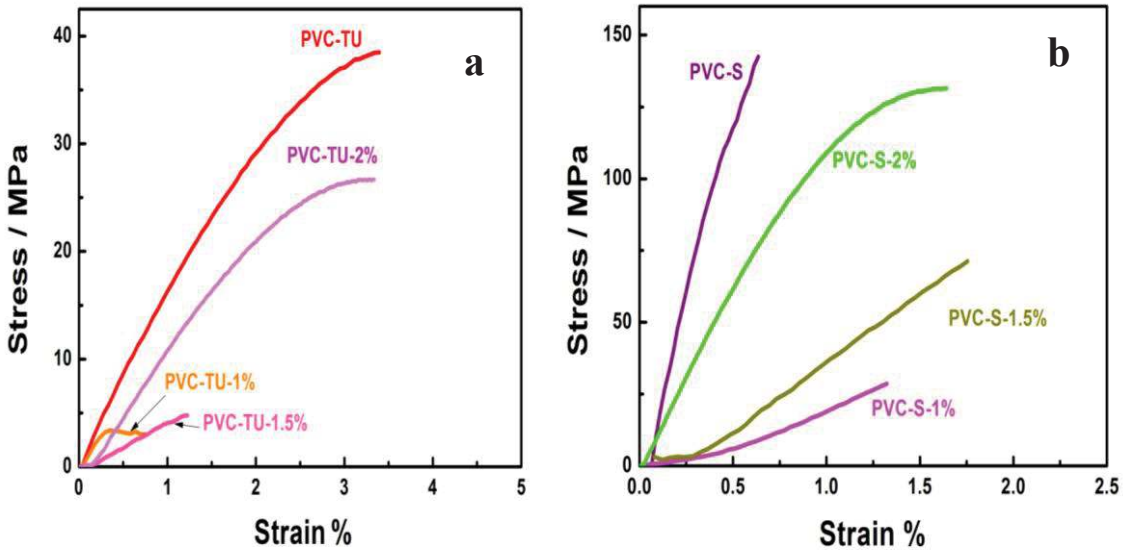

Figure 4.10: Stress strain curve of (a) PVC-TU and its different wt% of LDH nanocomposites; (b) PVC-S and its different wt% of LDH nanocomposite.

Apparently, the tensile strength and modulus tend to increase with increasing LDH amount. Such an increasing trend is more obvious for the tensile modulus. On the other hand, it also displayed excellent modulus and toughness. All the increase in the mechanical properties has been recorded in Table 4.3.

Stress Strain curve of PVC-TU and its composites has been shown in Figure 4.10 (a) which did not perform very well. PVC-TU-2% showed the highest ultimate strength compared to 1 & 1.5% but it was lower than PVC-TU. Tensile strength and tensile modulus decreases with increase in LDH wt% concentration. However, Wan *et al.* (2003) also compared the mechanical behaviour of PVC with organically modified MMT nano clay and found that intercalated material favours mechanical behaviour rather than exfoliation.

Table 4.4: Mechanical properties of PVC –TU and its different wt% nanocomposites

Sample	Modulus (GPa)	% Increase in Modulus	Toughness (kJm^{-3})	% Increase in toughness	Ultimate strength (UTS) (MPa)
PVC-TU	17.6		79.9	-	38.4
PVC-TU-1%	10.9	-38.0	1.93	-97.5	3
PVC-TU-1.5%	4.6	-73.8	2.8	-96.9	4.7
PVC-TU-2%	12.3	-30.1	53.9	-32.5	26.68

Stress Strain curve of PVC-S and its composites has been shown in Figure 4.10 (b) which also did not perform very well. PVC-S-2% showed the highest ultimate strength compared to 1 & 1.5% but it was lower than PVC-S. Tensile strength and tensile modulus decreases with increase in LDH wt% concentration.

Table 4.5: Mechanical properties of PVC –S and its different wt% nanocomposites

Sample	Modulus (GPa)	% Increase in Modulus	Toughness (kJm^{-3})	% Increase in toughness	Ultimate strength (UTS) (MPa)
PVC-S	320.1	-	46.6	-	142
PVC-S-1%	11	-96.5	15.01	-67.7	28.6
PVC-S-1.5%	49.5	-84.5	54.7	17.3	71.30
PVC-S-2%	76.0	-76.2	138.58	197.2	131.44

Tjong (2006) surveyed the mechanical properties of polymer–clay nanocomposites and concluded that these properties are highly correlated to their microstructure which is directly associated to the dispersion of clay platelets in the polymer matrix. More polymer insertion in the galleries of clay yields better mechanical behaviour which may be enhanced through different mixing method of clay into polymer matrix.

4.3 Summary

PVC/LDH, PVC-TS/LDH, PVC-TU/LDH and PVC-S/LDH composites with different weight percentage of LDH were obtained through solution intercalation method. The entire synthesized polymer composite presented improved thermal stability than the pure form. Mechanical testing studies showed that the polymer composites obtained from solution intercalation method have unassuming mechanical properties with no fixed pattern. This needs to be improved because polymer–clay nanocomposites exhibit extremely large interface due to the confinement of polymer chains within the galleries of clay platelets of large surface area per unit volume. It is considered that the confinement of polymer–clay interactions would affect the local chain dynamics to a certain extent. Since several chemical and physical interactions are governed by surfaces, polymer–clay nanocomposites can have substantially different properties from conventional polymer microcomposites.